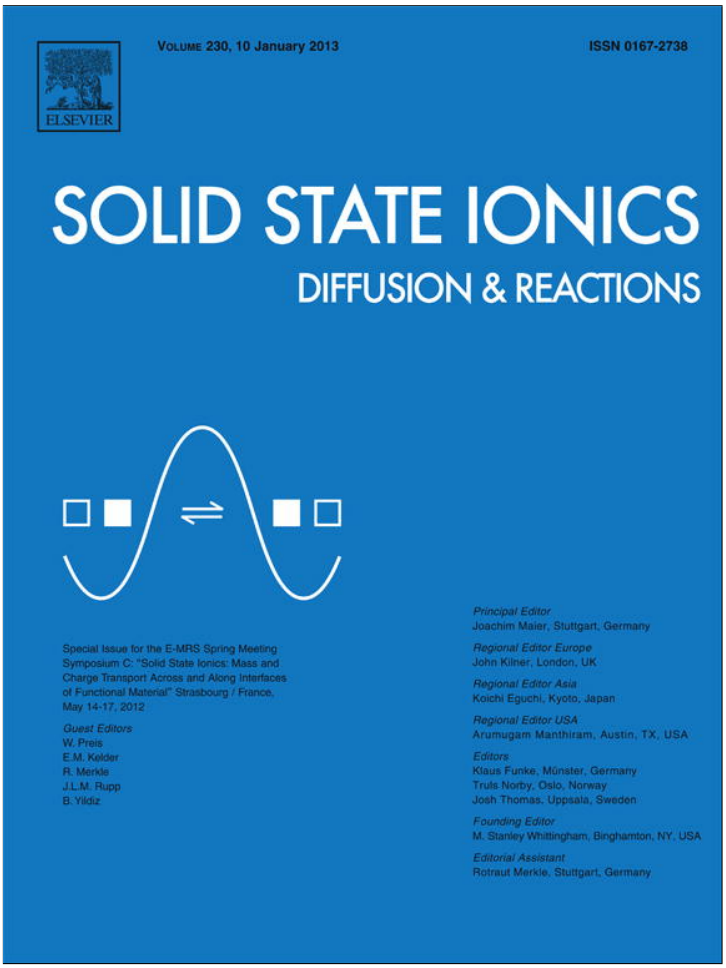

Solid State Ionics 230 (2013) 21–26

Contents lists available at SciVerse ScienceDirect

Solid State Ionics

journal homepage: www.elsevier.com/locate/ssi

First principles calculations of (Ba,Sr)(Co,Fe)$O_{3-\delta}$ structural stability

M.M. Kuklja [a,*], Yu.A. Mastrikov [b], B. Jansang [a], E.A. Kotomin [b,c]

[a] Department of Materials Science and Engineering, University of Maryland, College Park, MD 20742, USA
[b] Institute of Solid State Physics, University of Latvia, Kengaraga iela 8, Riga, LV 1063, Latvia
[c] Max Planck Institute for Solid State Research, Heisenbergstr. 1, D-70569, Stuttgart, Germany

ARTICLE INFO

Article history:
Received 1 May 2012
Received in revised form 22 August 2012
Accepted 27 August 2012
Available online 15 September 2012

Keywords:
Density functional theory
Defects
Disorder
Phase decomposition
Solid oxide fuel cells
Oxygen permeation membranes

ABSTRACT

First principles total-energy calculations of an ideal BSCF perovskite-type solid solution, the crystal containing basic point defects, and a set of relevant solid–solid solutions are presented. Our DFT modeling of defects (Frenkel, Schottky and cation exchange) and disordering in the BSCF perovskites reveals that the material tends to decompose at relatively low temperatures into a mixture of new perovskite and oxide phases. These new phases are likely to appear at grain boundaries and surface interfaces. This instability is predicted to negate advantages of fast oxygen transport chemistry and impede the applicability of BSCF-based SOFC and ceramic permeation membranes. We discuss possible mechanisms and origins of defect-induced (in)stability in the context of available experiments. This research explains the observed SOFC performance reduction, the significant scattering in the reported degree of oxygen nonstoichiometry, and provides insights on enhancing mass transport and energy conversion in SOFC and oxygen separation ceramic membranes.

Published by Elsevier B.V.

1. Introduction

The flexibility of the perovskite structure provides significant technological advantages for making fuel cell electrodes and gas separation membranes with improved efficiency. The perovskite ABO_3 lattice allows for a large variety of chemical elements to be used in designing the material and hence crafts a playground for achieving targeted mass and charge transport properties by manipulating chemical compositions. Among the many novel advanced materials for ecologically clean energy, ABO_3-type cubic perovskites and, especially, $(A_1A_2)(B_1B_2)O_3$ double perovskite solid solutions, e.g. $Ba_xSr_{1-x}Co_{1-y}Fe_yO_{3-\delta}$ (BSCF), are currently considered to be one of the most promising for applications as cathodes in solid oxide fuel cells (SOFC), oxygen permeation membranes [1–4], and oxygen evolution catalysis [5]. These perovskites exhibit good oxygen exchange performance, the highest oxygen permeation rates known for a solid oxide [1,6], and mixed ionic and electronic conductivity. The low oxygen vacancy formation energy and the relatively low activation barrier for the vacancy diffusion that are characteristic in these perovskites lead to the high oxygen vacancy concentration [7]. These factors largely define the fast oxygen reduction chemistry of these materials [8–10], which makes them such good candidates for energy conversion applications.

Experimental literature data for the oxygen nonstoichiometry of BSCF at a given temperature and oxygen partial pressure show considerable scatter with nonstoichiometric parameter δ ranging from 0.2 to 0.8, as summarized in [11]. An extraordinary ability of BSCF to accommodate oxygen vacancies without forming $ABO_{2.5}$ brownmillerite-type phase or other superstructures of highly ordered oxygen vacancies shows the highest oxygen nonstoichiometry observed to date for a cubic ABO_3 perovskite-type oxide [12]. Together with excellent properties, however, the flexibility of the perovskite lattice arrangement coupled with the high degree of oxygen nonstoichiometry leads to a serious disadvantage of BSCF, its slow transformation at intermediate temperatures into a mixture of several phases, including a hexagonal phase with strongly reduced performance [11–16].

The basic properties of these perovskites and their stability with respect to decomposition into several phases are governed by structural defects and disordering. At the moment the interplay between the chemical composition, structural order/disorder,[1] and crystalline stability in most perovskites is essentially unexplored because these materials are extraordinarily complex and especially difficult to tackle experimentally. Detailed knowledge of the structure–property–function relationship in BSCF and similar materials would ensure the rapid progress in energy research and open up new prospects to enhance existing materials or design novel materials for improved efficiency of energy conversion devices.

* Corresponding author. Tel.: +1 703 292 4940.
E-mail address: mkukla@nsf.gov (M.M. Kuklja).

[1] In this paper, terms defect(s) and disorder are often used as synonyms when they indicate any deviation from an ideal crystal arrangement of the perovskite structure.

0167-2738/$ – see front matter. Published by Elsevier B.V.
http://dx.doi.org/10.1016/j.ssi.2012.08.022

In this paper, aimed at understanding micro-scale origins of the BSCF lattice instability, a set of point defects, Frenkel and Schottky disorder, cation exchange, and solid-state decomposition reactions are explored in BSCF by means of first principles density functional theory (DFT) calculations. Reaction energies of those defects and disorder are carefully characterized and discussed in the context of available experimental data. It is established that oxygen Frenkel defects, full Schottky disorder and partial Schottky disorder accompanied by the growth of a new phase (e.g. a binary oxide) all have relatively low formation energies and are favorable. The obtained cation exchange energies are very low on both the A- and B-sublattices of the perovskite structure, while antisite defects (A ↔ B exchanges) are costly, which carries implications to the stability of the materials and ultimately to the efficiency of energy conversion. With computationally revealed details of possible disordering in BSCF and phase decomposition mechanisms that are difficult or impossible to attain from experiment alone, a consistent interpretation of the experimentally observed materials instability is suggested.

2. Details of calculations

The results were obtained by means of density functional theory (DFT) as implemented in the computer code VASP 4.6 [17] with Projector Augmented Wave (PAW) pseudopotentials and the exchange-correlation PBE functional of the GGA-type. We used the soft PAW PBE potential for O ions, which yields a binding energy for a free O_2 molecule very close to the experimental value and a reasonable O – O bond length (5.24 eV and 1.29 Å, cf. the experimental values of 5.12 eV and 1.21 Å, respectively [18]).

The original ideal supercells in our calculations were designed in such a way that the minimum anisotropy of the ionic distribution in the crystalline lattice is introduced. In other words, metals of the same chemical type were placed in the supercell as far from each other as possible to ensure the most uniform distribution of ions and the highest degree of the crystal isotropy. This tactic yields the BSCF model crystals (Fig. 1a) with the 50–50–75–25% composition, which simulates the closest to the most efficient BSCF 50–50–80–20% configuration determined experimentally.

Defects were simulated using large periodic supercells that were constructed by expanding the five-atom ABO_3-type cubic primitive unit cell by $2\times2\times2$ (40 atoms, used mostly for single defect calculations) and by $4\times4\times4$ (320 atoms, used for modeling Frenkel pairs and cation exchange). The $8\times8\times8$ k-point mesh in the Brillouin zone was used within the Monkhorst–Pack scheme [19] for the primitive ABO_3 unit cell, $4\times4\times4$ mesh for the 40 atom supercell and $2\times2\times2$ for the 320 atom supercell. The latter supercells were used in modeling the pair of Frenkel defects and cation structural disorder. Ionic charges were calculated by the Bader method [20]. The kinetic energy cut-off for the plane wave basis set was set to 520 eV. The basic properties of defect-free BSCF and oxygen vacancies therein are detailed in our previous publications [8,9,21]. In the calculations, the most common in experiments material composition $Ba_{0.5}Sr_{0.5}Co_{0.75}Fe_{0.25}O_3$ was modeled, unless indicated otherwise.

3. Discussion of the obtained results

Previously, it was established that the oxygen vacancy formation requires a considerably smaller energy E_V (~4 eV) [9,21] than cation vacancies (8.6–9.3 eV), all obtained with respect to isolated atoms [22]. The formation energy calculated with respect to 1/2 free O_2 molecule in the triplet state yields 1.34 eV for the oxygen vacancy placed between two Co atoms (Co–O–Co) and 1.40 eV between one Co and one Fe atom (Co–O–Fe) [9,22]. These energies are significantly smaller than those for a wide-gap perovskite-prototype $SrTiO_3$ (ca. 6 eV) [23] and even for $La_{0.75}Sr_{0.25}MnO_3$ (2.7 eV) [24,25] used in SOFC applications.

Table 1 lists the formation energies for well-separated defect pairs and shows that among the Frenkel defects, the oxygen vacancy–interstitial pairs have the lowest energy of ~0.75–0.89 eV per defect with some preference given to the oxygen vacancy placed between two Co atoms in the BSCF lattice rather than between one Co and one Fe atom. This is in agreement with the formation energies of the respective single oxygen vacancies. Note that the formation energies for oxygen Frenkel defects in BSCF turn out to be much smaller than in other relevant perovskites, e.g. $SrTiO_3$ (~10 eV) [26] and $LaFeO_3$ (~4 eV) [27], which translates into a much higher equilibrium concentration of defects. Both the *split* and *hollow* configurations were probed for interstitial atoms (Fig. 1) for close (~5 Å) and distant (>15 Å) interstitial–vacancy pairs calculated within the same large supercells. The close pairs are shown only for the oxygen Frenkel defects (see the energies in parentheses in Table 1), the energies of which only slightly differ from the distant pairs. Interstitial defects cause a significant lattice distortion and redistribution of the electronic density, as illustrated in Fig. 1.

It was also recognized that the full canonical Schottky disorder and Schottky-like examples of a possible change in the chemical composition of the material (partial Schottky disorder) have unusually low energies, 0.73–1.48 eV per defect [22]. Although the partial Schottky defects accompanied by the formation of binary oxides require somewhat larger energies, 1.40–1.48 eV, than the formation of perovskites, 0.73–0.86 eV, those energies are low enough to expect an efficient formation of binary oxides also at grain boundaries [22]. We note that full Schottky and Schottky-like disorders as well as Frenkel disorder are favorable, with some preference given to the vacancy disorder. The calculated energies suggest that the fairly high cation vacancy formation energies (8.6–9.3 eV) are balanced by extremely low oxygen vacancy formation energies (1.34 eV with respect to atoms in O_2 gas phase molecule) [22]. This implies that the presence of cation vacancies in BSCF, which results in an appearance of mobile atoms, will lead to the nucleation and growth of new perovskites or oxides, also meaning that grain boundaries and BSCF surfaces should favor parent ABO_3 compositions.

This assumption is convincingly verified by recent Scanning Electron Microscopy (SEM) and Transmission Electron Microscopy (TEM) measurements, revealing that the new hexagonal phase grows predominantly at the grain boundaries of BSCF ceramics and that the cation composition of the newly formed hexagonal phase differs from that of the starting material [13,14]. It is clear that the efficiency of crystallization into a new phase will depend not only upon the favorable thermodynamics – the reaction energy (which is low, as demonstrated above), but also upon the kinetics – the reaction rate, which, in turn, is a strong function of the activation barriers for the cation diffusion and their rates. Cations in perovskites tend to migrate much slower than oxygen [28]. Hence, we expect that the process of a new phase transformation is fairly slow as compared to the oxygen chemistry. Note that oxygen vacancy formation energy is considerably reduced with the temperature increase due to a decrease of the oxygen chemical potential [18]. This reduction could be $\Delta G \approx 1$ eV while temperature increases from room to 1200 K (operational temperature of the solid oxide fuel cell) [29]. As a result, the formation energy of oxygen vacancies at high temperatures becomes much smaller than Frenkel or Schottky defects, which leads to a strong deviation of BSCF from oxygen stoichiometry [2].

Not surprisingly, another manifestation of the predicted self-segregation was found in the cation clustering effect, or $A_1 \leftrightarrow A_2$ and $B_1 \leftrightarrow B_2$ cation exchange, e.g. exchanging one Ba with one Sr in the supercell results in the aggregation of the Sr and Ba perovskite phases. We found that the cation exchange on either the A- or B-sublattices of the ABO_3 perovskite lattice requires a negligible energy. From the energetic point of view, this indicates that both the A metals (Ba and Sr) and the B metals (Co and Fe) can be almost randomly dissolved on the respective sublattices [22]; this is in agreement with earlier calculations [30]. This conclusion lends strong support

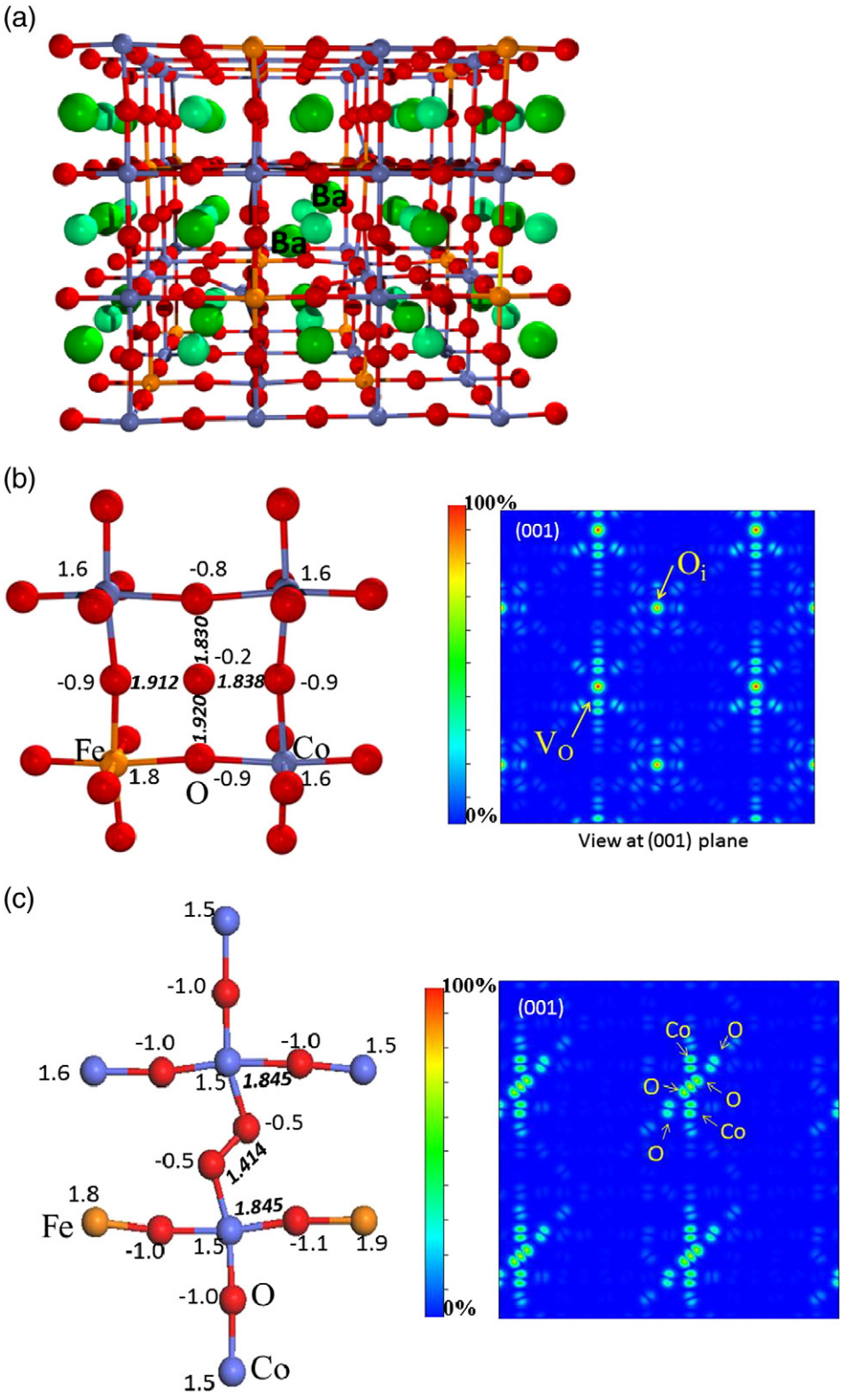

Fig. 1. (a) Ba–Ba split interstitial defect in the BSCF crystalline lattice and (b) details of oxygen hollow and (c) Co–O–Co oxygen split interstitial configuration, with the atomic charges, interatomic distances, and the differential electronic density map are shown.

to the high tolerance of the cubic polymorph towards the A-site and B-site compositions suggested based on TEM images and Selected Area Electron Diffraction (SAED) patterns of cubic and hexagonal BSCF [14]. At the same time, antisite substitutions (A ↔ B cation exchange, for example, Sr ↔ Co), while possible, are quite costly, 3.79–7.87 eV. They require a significantly higher energy than the clustering of cations within the same sublattice due to the need for charge compensation, the difference in ionic radii of the A and B atoms, and the different site coordination numbers in the ideal crystalline lattice. Bearing in mind that the cation diffusion is relatively slow, the antisite defects can be hardly considered as a favorable disorder in BSCF.

Table 1
Vacancy–interstitial pair (Frenkel disorder) formation energies are described in standard Kröger and Vink notations and calculated (per defect) for stoichiometric material. The effects of higher oxygen vacancy concentrations were studied in ref. [9].

N	Frenkel pair	Interstitial configuration	Formation energy[a] [eV]
(1)	$Ba_{Ba}^{x} \leftrightarrow V_{Ba}'' + Ba_i^{\cdot\cdot}$	Split	6.02
(2)	$Sr_{Sr}^{x} \leftrightarrow V_{Sr}'' + Sr_i^{\cdot\cdot}$	Split	4.49
(3)	$Co_{Co}^{x} \leftrightarrow V_{Co}'' + Co_i^{\cdot\cdot\cdot\cdot}$	Hollow	1.76
(4)	$Fe_{Fe}^{x} \leftrightarrow V_{Fe}'' + Fe_i^{\cdot\cdot\cdot\cdot}$	Hollow	2.41
(5)	$O_O^{x} \leftrightarrow V_{Co-O-Co}^{\cdot\cdot} + O_i''$	Split	0.75 (0.76)[b]
		Hollow	1.85 (1.86)
(6)	$O_O^{x} \leftrightarrow V_{Co-O-Fe}^{\cdot\cdot} + O_i''$	Split	0.89 (0.91)
		Hollow	1.88 (1.89)

[a] Energies are given for well-separated defects placed within the same large supercell.
[b] The energies in parentheses correspond to the close pairs of the oxygen Frenkel defects and show that they only slightly differ from the distant pairs.

With the astounding ability of the BSCF crystalline lattice to accommodate a variety of disorder scenarios, the most challenging and the most intriguing part of this work aims at elucidation of the micro-scale origins of phase stability, which has implications for ionic and electronic conductivity, energy conversion, and, in turn, for the device (SOFC, membranes, and reactors) performance. An additional advantage of this computational modeling strategy is provided by its capacity to determine effects of high oxygen deficiency on the cubic and hexagonal phase decomposition, which are extremely difficult to obtain from experiment alone (see for example, [11]).

Our DFT calculations of ideal, stoichiometric in oxygen BSCF structures at 0 K predict that the hexagonal BSCF crystal phase is 0.66 eV per formula lower in energy than the cubic phase. Note that practical nonstoichiometric BSCF samples rest on the cubic-hexagonal stability border, and at high temperatures the crystal maintains its cubic structure [14]. An estimate based on the kinetic data [14] shows that for the longest cooling times of around 15 min, the phase fraction of the hexagonal phase was 1% or lower and thus negligible at the point at which equilibrium of the oxygen sublattice of the parent cubic phase was attained [11]. Nevertheless, the TGA temperature jump experiments confirm co-existence of both phases in the BSCF samples (Fig. 6 in ref. [11]) and lend some additional validation to our results. We demonstrate below that the oxygen vacancies indeed stabilize the cubic phase; total energies of both phases are close to each other at oxygen nonstoichiometries observed experimentally ($\delta \approx 0.75$).

To relate our modeling to real crystals and experimental observations, we simulated oxygen nonstoichiometry in the model $Ba_xSr_{1-x}Co_{0.75}Fe_{0.25}O_{3-\delta}$ composition in both cubic and hexagonal (2H) phases (Fig. 2) by varying the δ parameter in a wide range from 0 to 1 (0–30% of oxygen sites are vacant), as illustrated in Fig. 3. Several important conclusions immediately follow from this modeling. First, total energy calculations demonstrate that the presence of oxygen vacancies stabilizes the cubic phase, which becomes energetically more favorable

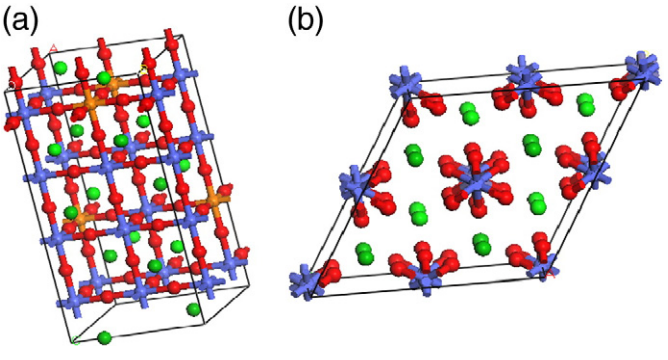

Fig. 2. Schematic view of the supercells of the a) cubic and b) hexagonal (2H) BSCF perovskite structures.

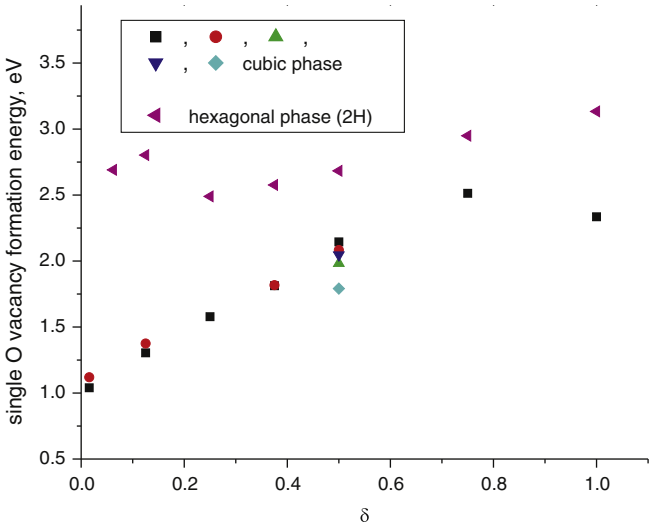

Fig. 3. The single vacancy formation energy of the cubic and hexagonal phases of BSCF is shown as a function of oxygen non-stoichiometry parameter δ. Five points shown for $\delta = 0.5$ demonstrate the energy dispersion depending upon a spatial distribution of vacancies in the crystal.

than the hexagonal phase at $\delta > 0.75$. We note here that the close matching between theoretical and experimental results of the BSCF lattice parameters was also achieved only with the oxygen vacancies and the corresponding lattice expansions included in the calculations [8,21]. Second, the formation energy of oxygen vacancies in the cubic phase is considerably smaller than in the hexagonal phase (Fig. 3), which translates into a significantly higher defect concentration expected in the cubic BSCF. The revealed difference offers a simple explanation to high scatter of δ parameter reported in experimental studies [11]. The absolute value of δ parameter is lower in the hexagonal phase than in the cubic phase. Neglect of this fact and of possible BSCF decomposition into other phases and other oxides (vide infra), which also have various degrees of oxygen deficiency accommodated in the lattices, would lead to significant errors of δ ascribed to samples in the experiment. Third, unlike the hexagonal phase, the defect formation energy strongly increases in the cubic phase with the defect concentration, which limits the vacancy accumulation.

Two imperative observations obtained from our modeling, the low energy of the new phase growth (or self-segregation) coupled with the low energy of the cation substitutions within the A or B sublattice (or high cation miscibility), evidently point to the possible decomposition of BSCF into other solid solutions or parent perovskites. Hence, we explored a large set of possible decomposition reactions for both cubic and hexagonal phases and two extreme stoichiometry parameters, $\delta = 0$ and $\delta = 1$; only a few select reactions are shown in Table 2. Stable oxides of this nonstoichiometry ($\delta = 1$) are known to exist, for instance, $SrFeO_2$, $BaCoO_2$, and $CaFeO_2$ [11]. $SrFeO_2$ and $CaFeO_2$ can be obtained by reducing $SrFeO_{3-\delta}$ or $CaFeO_{3-\delta}$, respectively, with CaH_2 [31,32]. Thus, Eq. (1) describes a decomposition of $Ba_xSr_{1-x}Co_{0.75}Fe_{0.25}O_{3-\delta}$ ($x = 0.5$) into Ba- and Sr-rich perovskites, $BaCo_{0.75}Fe_{0.25}O_3$ and $SrCo_{0.75}Fe_{0.25}O_3$ ($x = 1, 0$). The energy of this reaction that imitates the ultimate separation of A cations (or the maximum extent of Ba and Sr clustering) in BSCF is close to zero or negative. In a similar way, Eq. (2) describes a full partition of $Ba_{0.5}Sr_{0.5}Co_{1-y}Fe_yO_{3-\delta}$ ($y = 0.25$) into *hexagonal* $Ba_{0.5}Sr_{0.5}CoO_3$ cobaltite and *cubic* $Ba_{0.5}Sr_{0.5}FeO_3$ ferrate ($y = 0, 1$) perovskite phases, which yields an energy gain of −0.56 eV for the cubic BSCF phase and a small reaction energy of 0.09 for the hexagonal phase. This indicates that in both stoichiometric phases, the BSCF material is unstable. An incorporation of high concentration of oxygen vacancies ($\delta = 1$) makes the reaction even more exothermic as the initial defective BSCF crystal is higher in energy, as compared to the ideal material. We stress here that in

Table 2
Energies of select decomposition reactions of cubic and hexagonal stoichiometric BSCF ($Ba_{0.5}Sr_{0.5}Co_{0.75}Fe_{0.25}O_{3-\delta}$ with $\delta=0$) and the material containing oxygen vacancies ($Ba_{0.5}Sr_{0.5}Co_{0.75}Fe_{0.25}O_{3-\delta}+1/2O_2$ with $\delta=1$) are calculated at 0 K and normalized per formula unit. An entropy contribution is neglected in calculations. A negative energy indicates an exothermic reaction.

N	BSCF phase decomposition reaction	Energy per formula unit [eV]			
		Cubic		Hexagonal	
		$\delta=0$	$\delta=1$	$\delta=0$	$\delta=1$
(1)	BSCF ↔ $1/2BaCo_{0.75}Fe_{0.25}O_3+1/2SrCo_{0.75}Fe_{0.25}O_3$	−0.01	−2.34	0.65	−2.49
(2)	BSCF ↔ $3/4Ba_{0.5}Sr_{0.5}CoO_{3(hex)}+1/4Ba_{0.5}Sr_{0.5}FeO_{3(cub)}$	−0.56	−2.90	0.09	−3.04
(3)	BSCF ↔ $1/4[BaCoO_3+SrCoO_3+Ba_{0.5}Sr_{0.5}CoO_3+Ba_{0.5}Sr_{0.5}FeO_3]$	−0.29	−2.62	0.37	−2.76
(4)	BSCF ↔ $1/4[BaO_2+SrO+Co_2O_3+Ba_{0.5}Sr_{0.5}CoO_3+Ba_{0.5}Sr_{0.5}FeO_3]$	−0.13	−2.46	0.53	−2.60
(5)	BSCF ↔ $1/2BaCoO_{3(hex)}+1/4SrCoO_3+1/4SrFeO_{3(cub)}$	−0.18	−2.51	0.48	−2.65
(6)	BSCF ↔ $1/4BaCoO_{3(hex)}+1/2SrCoO_3+BaFeO_{3(hex)}$	−0.03	−2.36	0.63	−2.50
(7)	BSCF ↔ $1/4[BaO_2+Co_2O_3+BaCoO_{3(hex)}+SrO+SrFeO_{3(cub)}]$	−0.01	−2.35	0.64	−2.49
(8)	BSCF ↔ $1/4[2BaO_2+Co_3O_4+SrO+SrFeO_3]$	0.53	−1.81	1.18	−1.95
(9)	BSCF ↔ $1/4[BaCoO_3+SrCoO_3+SrO+BaO+1/2Co_2O_3+1/2Fe_2O_3]$	1.62	−0.71	2.28	−0.86
(10)	BSCF ↔ $1/4[BaO+BaCoO_3+Co_2O_3+2SrO+FeO]$	3.08	0.75	3.74	0.61

the nonstoichiometric case, the reaction energetics is a function of temperature. The oxygen formation energy of BSCF containing defects decreases with the temperature increase due to entropy effects [25], and therefore the reaction energy would increase by the same amount. For example, taking into account a reduction in energy of ≈1 eV of the oxygen chemical potential as temperature increases from room temperature to 1200 K (see, ref. [18,29]) results in the reaction energy of cubic BSCF becoming −1.9 eV rather than −2.9 eV (Eq. (2), $\delta=1$ in Table 2) that still remains negative.

A fraction of resultant $Ba_{0.5}Sr_{0.5}CoO_{3(hex)}$ material can suffer further decomposition into two parent perovskites (Eq. (3)) or even further into three binary oxides (Eq. (4)). The BSCF decomposition into three parent perovskites is also energetically favorable (Eqs. (5) and (6) in Table 2); and variations of combined oxide and perovskite phases can appear as products as well (Eqs. (7)–(10)). The noticeable trend is that the smaller portion of the material stays in the perovskite structure and the larger portion assumes oxide compositions, the higher reaction energy is required. A complete phase separation into oxides (rather than perovskites or oxide–perovskite combinations) is unlikely for both cubic and hexagonal stoichiometric BSCF (largely due to mass and charge imbalance) and becomes possible only for strongly nonstoichiometric crystals, the corresponding energies for these decomposition routs are quite high though.

The separation into the respective phases is in qualitative agreement with SEM, TEM, SAED, and XRD experimental observations [14] and consistent with the observed slow phase transition or decomposition of BSCF into Ba-substituted $Sr_6Co_5O_{15}$ with enlarged lattice constants, an iron-substituted Co_3O_4, and a hexagonal perovskite with a 2H stacking sequence [15] (see also [4,11]). The decomposition of the cubic BSCF5582 at temperatures below 1173 K into hexagonal and cubic perovskite phases of significantly different cation compositions and oxygen nonstoichiometries was also proposed to proceed in accordance with equation[11,14]:

$$Ba_{0.5}Sr_{0.5}C_{0.8}F_{0.2}O_{3-\delta} \leftrightarrow 1/2Ba_{0.5+x}Sr_{0.5-x}CoO_{3-\delta(hex)} + 1/2Ba_{0.5-x}Sr_{0.5+x}Co_{0.6}Fe_{0.4}O_{3-\delta(cub)}.$$

Fundamentally, the equation resembles Eqs. (1) and (2) in Table 2, given minor differences in the chemical composition of experimental $Ba_{0.5}Sr_{0.5}C_{0.8}$ $F_{0.2}O_{3-\delta}$ and our model $Ba_{0.5}Sr_{0.5}C_{0.75}$ $F_{0.25}O_{3-\delta}$ samples. In addition to these mechanisms, Table 2 suggests many other possible decomposition routs with favorable thermodynamics.

Strictly speaking, appropriate caution should be exercised when a direct comparison of the calculated energies to available experiments is attempted because: (i) the relative stability of possible phases strongly depends not only on defect content, but also on their cation compositions [11,14,15] and (ii) possible nonstoichiometry of the products in the decomposition reactions (Table 2) is neglected in our modeling. The entropy effects in the defect formation under realistic experimental conditions (high temperatures and realistic gas pressure) were discussed, e.g. in ref. [25], and the temperature effects on decomposition reactions could be treated, for example, by using a thermodynamic approach suggested in ref. [33]. Nevertheless, qualitative agreement between our theoretical predictions and experimental observations remains valid, and, most importantly, the analysis based on DFT total energy calculations allows us to foresee the behavior of complex perovskite solid solutions with no a priori assumptions, and therefore, our calculations can aid in the interpretation of experiments and the design of further studies.

4. Conclusions

A range of point defects and select relevant solid-solution chemical reactions were explored by means of ab initio DFT calculations performed by using large supercells and a variety of ideal and defective BSCF related crystalline structures. We established that the complexity of the BSCF crystalline arrangement leads to a possibility of accommodating many variations of point defects in the lattice and determines its chemical instability. Cation clustering in the A-sublattice (exchange of Sr and Ba positions) or B-sublattice (exchange of Co and Fe positions) requires a low energy, implying that the distribution of metals in the BSCF lattice is not necessarily highly ordered. This behavior considerably differs from dopant ordering predicted theoretically for Sr in $LaMnO_3$ [33] and observed experimentally for Sr in $LaCoO_3$ [34].

Unlike cation clustering, the formation of A ↔ B antisite (Ba ↔ Fe) defects is energetically costly and hardly contributes to disorder. Oxygen Frenkel defects, Schottky defects, and partial Schottky-like disorder coupled with the growth of new material phases and oxygen vacancies all exhibit unusually low formation energies, with some preference given to the vacancy disorder due to a considerable decrease of the oxygen vacancy formation energies with the temperature increase [29]. Consequently, due to entropy effects, the oxygen vacancy formation energy decreases with the temperature even more, which makes vacancy defects predominant in BSCF at the SOFC operational temperatures, in agreement with experiment.

We have demonstrated that a high concentration of oxygen vacancies serves to stabilize the BSCF cubic phase in which their formation energies are considerably smaller than those in the hexagonal phase. The difference in the vacancy formation energies in two phases offers an explanation to the large dispersion of δ measured experimentally. We also established that the vacancy formation energy in the cubic phase appreciably increases with the material's non-stoichiometry.

Undoubtedly, the reason for the different behavior of the defect formation energy in the two phases deserves a further investigation.[2]

Based on energetic considerations, both oxygen-stoichiometric and vacancy containing BSCF are thermodynamically unstable and hence are expected to decompose *at low temperatures* into a mixture of several cubic and hexagonal perovskite phases via several alternative routes. This process depends on a delicate balance between a thermodynamic trend for segregation with a decrease of temperature and a sharp slowdown of the kinetics of this process in BSCF [14]. This translates into the narrow temperature window (~800–900 °C for BSCF) where the hexagonal phase is indeed experimentally observed [11].

The new perovskite phases are predicted to nucleate and grow, most likely, on grain boundaries or surfaces of BSCF, plenty of which are available, for example, in porous cathodes of SOFC. This will significantly impede the efficiency of BSCF based fuel cell cathodes, separation membranes, and catalysts largely due to the less advantageous oxygen chemistry in those resultant materials. The obtained conclusions are consistent with experimental observations and could help for future reliable predictions of the behavior of other relevant candidate materials (e.g. LSCF) under realistic operational conditions.

Acknowledgments

Authors are greatly indebted to R. Merkle, J. Maier, D. Fuks, R. A. De Souza, J. Caro, D. Gryaznov, and A. Roytburd for many stimulating discussions. This research was supported in part by the German-Israeli Foundation grant no. 1025-5.10/2009, National Science Foundation (NSF) grant CMMI-1132451, and DOE Contract DE-AC02-05CH11231, supporting NERSC resources. MMK is grateful to the Office of the Director of NSF for support under the IRD program. Any appearance of findings, conclusions, or recommendations, expressed in this material are those of the authors and do not necessarily reflect the views of NSF.

References

[1] Z. Shao, S.M. Haile, Nature 431 (2004) 170.
[2] L. Wang, R. Merkle, J. Maier, J. Electrochem. Soc. 157 (2010) B1802.
[3] W. Zhou, R. Ran, Z. Shao, J. Power Sources 192 (2009) 231.
[4] F. Liang, H. Jiang, H. Luo, J. Caro, A. Feldhoff, Chem. Mater. 23 (2011) 4765–4772.
[5] J. Suntivich, K.J. May, H.A. Gasteiger, J.B. Goodenough, Y. Shao-Horn, Science 334 (6061) (2011) 1383–1385.
[6] Z. Shao, W. Yang, Y. Cong, H. Dong, J. Tong, G. Xiong, J. Membr. Sci. 172 (2000) 177.
[7] L. Wang, R. Merkle, J. Maier, ECS Trans. 25 (2009) 2497.
[8] Yu.A. Mastrikov, M.M. Kuklja, E.A. Kotomin, J. Maier, Eng. Environ. Sci. 3 (2010) 1544.
[9] E.A. Kotomin, Yu.A. Mastrikov, M.M. Kuklja, R. Merkle, A. Roytburd, J. Maier, Solid State Ionics 188 (2011) 1.
[10] F.S. Baumann, J. Fleig, H.-U. Habermeier, J. Maier, Solid State Ionics 177 (2006) 3187–3191.
[11] D. Mueller, R.A. De Souza, H.I. Yoo, M. Martin, Chem. Mater. 24 (2012) 269–274.
[12] S. McIntosh, J.F. Vente, W.G. Haije, D.H.A. Blank, H.J.M. Bouwmeester, Chem. Mater. 18 (2006) 2187–2193.
[13] S. Svarcova, K. Wiik, J. Tolchard, H.J.M. Bouwmeester, T. Grande, Solid State Ionics 178 (2008) 1787.
[14] D.N. Mueller, R.A. De Souza, T.E. Weirich, D. Roehrens, J. Mayer, M. Martin, Phys. Chem. Chem. Phys. 12 (2010) 10320–10328.
[15] R. Kriegel, R. Kircheisen, J. Töpfer, Solid State Ionics 181 (2010) 64.
[16] K. Efimov, Q. Xu, A. Feldhoff, Chem. Mater. 22 (2010) 5866–5875.
[17] G. Kresse, J. Furthmueller, VASP the Guide: Univ. Vienna, 2003.
[18] NIST Computational Chemistry Comparison and Benchmark Database, 14th ed., Am. Chem. Soc., Washington, 2006.
[19] H.J. Monkhorst, J.D. Pack, Phys. Rev. B 13 (1976) 5188.
[20] G. Henkelman, A. Arnaldsson, H. Jónsson, Comp. Mater. Sci. 36 (2006) 254.
[21] R. Merkle, Yu.A. Mastrikov, E. Kotomin, M.M. Kuklja, J. Maier, J. Electrochem. Soc. 159 (2012) B212–B226.
[22] M.M. Kuklja, Yu.A. Mastrikov, B. Jansang, E.A. Kotomin, J. Phys. Chem. C. 116 (35) (2012) 18605–18611, http://dx.doi.org/10.1021/jp304055s.
[23] Y.F. Zhukovskii, E.A. Kotomin, R.A. Evarestov, D.E. Ellis, Int. J. Quantum Chem. 107 (14) (2007) 2956–2985.
[24] S. Piskunov, E. Heifets, T. Jacob, E.A. Kotomin, D.E. Ellis, E. Spohr, Phys. Rev. B 78 (2008) 121406.
[25] Y.A. Mastrikov, R. Merkle, E. Heifets, E.A. Kotomin, J. Maier, J. Phys. Chem. C 114 (7) (2010) 3017–3027.
[26] B.S. Thomas, N.A. Marks, B.D. Begg, Nucl. Inst. Methods B 254 (2007) 211.
[27] A. Jones, M.S. Islam, J. Phys. Chem. C 112 (2008) 4455–4462.
[28] J.X. Yi, H.L. Lein, T. Grande, S. Yakovlev, Solid State Ionics 180 (2009) 1–5.
[29] R. Evarestov, E. Blokhin, D. Gryaznov, E.A. Kotomin, R. Merkle, J. Maier, Phys. Rev. B 85 (2012) 174303.
[30] S. Gangopadhayay, T. Inerbaev, A.E. Mansurov, D. Altilio, N. Orlovskaya, Appl. Mater. Interfaces 1 (2009) 1512–1519.
[31] Y. Tsujimoto, C. Tassel, N. Hayashi, T. Watanabe, H. Kageyama, K. Yoshimura, M. Takano, M. Ceretti, C. Ritter, W. Paulus, Nature 450 (2007) 1062–1065.
[32] S. Inoue, M. Kawai, N. Ichikawa, H. Kageyama, W. Paulus, Y. Shimakawa, Nat. Chem. 2 (2010) 213–217.
[33] D. Fuks, L. Bakaleinikov, E.A. Kotomin, J. Felsteiner, A. Gordon, R.A. Evarestov, D. Gryaznov, J. Maier, Solid State Ionics 177 (2006) 217–222.
[34] Z.L. Wang, J. Zhang, Phys Rev B 54 (1996) 1153.

[2] We would like to stress here that the instability found in the reactions in Table 2 has implications for preparing BSCF crystals. The discussion of possible synthesis conditions, which certainly deserves a further consideration, is well beyond the scope of this short article, so we refer readers to our much more detailed thermodynamic study of the entropy effects at high temperatures, which will be reported elsewhere.